JOURNAL OF MATERIALS SCIENCE 27 (1992) 661–670

# Electron microdiffraction studies of zirconia particles

R. SRINIVASAN, B. H. DAVIS
*Center for Applied Energy Research, 3572 Iron Works Pike, Lexington, KY 40511, USA*

L. A. RICE
*Department of Materials Science and Engineering, University of Kentucky, Lexington, KY 40506, USA*

R. J. de ANGELIS
*Center for Materials Research and Analysis, University of Nebraska at Lincoln, Lincoln, NE 68588, USA*

A batch of zirconia was prepared at a pH of 2.95 using a sol-gel technique. The crystal structures formed during 500 °C calcination was followed by X-ray diffraction. The tetragonal phase was the major component after the initial calcination period of 15.5 h; however, it gradually transformed to the monoclinic crystal form during 200 h of calcination at 500 °C. Electron microdiffraction was employed in the present investigation to determine the crystal structure of individual particles, and to identify whether these particles contained twin variants. A technique has been developed to get a dispersion of agglomerated particles by condensing and spreading the beam on the agglomerates at 200 kV. The data revealed that some of the individual zirconia particles are featureless and some of them appear to contain single or multiple twin variants.

## 1. Introduction

Zirconia is an industrially important ceramic material. It is used in a wide range of areas which includes catalysis, sensor applications, gas turbines, magnetic hydrodynamics process of power generation, thermal barrier coatings, high temperature nozzles in air engines, etc. The versatility of zirconia makes it a viable candidate for sophisticated and robust engineering applications.

Zirconia exhibits polymorphism [1–6]; i.e., it exists in three different crystalline forms, namely monoclinic, tetragonal and cubic [7]. Recently another high pressure orthorhombic form of zirconia has been reported [8]. The transition from the tetragonal phase to the monoclinic phase has great importance in industrial applications for this material. The monoclinic form transforms to tetragonal structure at about 1150 °C and the *t*-phase reverts to *m*-phase at about 950 °C on cooling. This reversible $t \leftrightarrow m$ transformation is termed martensitic, just as the case may be in Transformation Induced Plasticity (TRIP) steels [9, 10]. As a result of this transformation a volume expansion and a shape change occur as the tetragonal lattice expands to a larger monoclinic lattice. The volume expansion offers a compressive force in the crack-tip stress field, so that the propagation of cracks is arrested. Thus, the mechanical properties such as resistance to mechanical failure are greatly improved.

To stabilize the high temperature *t*-phase at temperatures as low as room temperature, compounds such as CaO, $Y_2O_3$, MgO are commonly added to zirconia in appropriate proportions. There are two forms of stabilized zirconias, namely partially stabilized (PSZ) zirconia and fully stabilized zirconia (FSZ). The PSZ's are known to display better mechanical properties [10].

The tetragonal structure of the unstabilized pristine zirconia can be stabilized at low temperatures by controlling chemical factors involved in the precipitation process [11]. The pH of the precipitation of zirconia from its salts appears to determine the crystal structure of the material after calcination at 400–600 °C [11]. Also the stability of the phases formed after calcination at 500 °C has been investigated in detail [12, 13].

Earlier reports [12] indicated that the tetragonal phase of $ZrO_2$, precipitated at pH 2.95, gradually transforms to monoclinic phase at 500 °C with increasing calcination time. The X-ray diffraction particle size data revealed that tetragonal crystallite size decreases during transformation to the monoclinic phase. This could be due to one tetragonal particle transforming to a smaller monoclinic particle possibly due to twinning or the existence of other defects produced during the transformation. These possibilities are the focus of the present investigation. The main objective of the current investigation is to find the reasons for the decrease in the diffracting particle size which occurs during the $t \rightarrow m$ transformation. To accomplish this a technique was developed to isolate

0022–2461/92 $03.00 + .12 

the very small particles from their agglomerates. Then 2 and 5 nm probes have been utilized to obtain electron microdiffraction patterns from the isolated ultrafine zirconia particles.

## 2. Experimental procedure

### 2.1. Preparation of Zirconia

A solution of 0.3 M $ZrCl_4$ was precipitated using $NH_4OH$ at a pH of 2.95. After washing the gels thoroughly up to peptization, they were dried at 120 °C, overnight. The dried gels were then calcined in a muffle furnace at 500 °C, withdrawing samples at 15.5, 50, 100, 150 and 200 h.

### 2.2. Transmission Electron Microscopy and Microdiffraction

Microdiffraction was used to study the crystalline structure of particles between 1–30 nm diameter on an individual basis. Microdiffraction makes it possible to obtain precise crystallographic information from individual particles which could not be obtained by selected area electron diffraction (SAED). The transmission electron microscopy (TEM) work was carried out using a Hitachi H800 NA microscope operating at 200 kV. Electron microdiffraction data were obtained in the conventional transmission mode using electron probes of 2 and 5 nm in diameter.

The TEM samples were prepared by suspending the particles of calcined zirconia samples in absolute alcohol. After attaining the optimum ratio of alcohol to powder particles such that the particles are suspended in a slightly turbid solution, the suspension was constantly agitated in an ultrasonic bath. A drop of this suspended solution was placed on a carbon-coated formvar film predeposited on a copper grid. After the absolute alcohol evaporated leaving the small particles on the grid, the specimen was loaded into the microscope for analysis. A description of samples observed in an earlier study [12] is given in Table I.

A procedure is needed to get fine individual particles from the agglomerated lumps so that the electron microdiffraction technique is useful in obtaining microdiffraction data. If the beam coming through the condenser lens is spread and condensed several times over an agglomerate, the fine particles which would otherwise cling together are separated and thrown around the lump. It then becomes easy to locate these ultrafine individual particles with the probe and obtain microdiffraction patterns of single particles. Microdiffraction from individual particles were obtained after pulsing the beam on lumps to cause separation. This phenomenon was observed serendipitously during unsuccessful experiments designed to produce individual particles. During these experiments, we observed small particles around the lumps and then a systematic procedure to get a dispersion of the particles was developed. The appearance of a number of small particles around a lump is shown in Fig. 1. The micrograph in Fig. 1a shows the lump before pulsing the beam using a condenser, and the micrograph in Fig. 1b depicts the situation after pulsing the beam six times. A number of ultrafine individual particles exist in the region around the lump. Thus, we are able to obtain individual particles for further investigation.

TABLE I Specifications of zirconia samples prepared at a pH of 2.95 and calcined at 500 °C

| Sample | Calcination time (h) | Tetragonal phase[a] (%) |
|---|---|---|
| A | 15.5 | 80 |
| B | 50 | 45 |
| C | 100 | 35 |
| D | 150 | 25 |
| E | 200 | 15 |

[a] Determined from the X-ray diffraction patterns; remainder is the monoclinic phase.

## 3. Results and discussion

### 3.1. Experimental results

Bright and dark field observations along with electron microdiffraction patterns were obtained from various subnanometer particles of zirconia from the calcination conditions given in Table I. These observations are presented in the following section with brief descriptions of associated features.

#### *3.1.1. Sample A*

This sample, calcined at 500 °C for 15.5 h, was found to contain about 80 vol % tetragonal phase by X-ray diffraction (XRD). A typical bright field electron micrograph obtained from this sample is shown in Fig. 2. It is evident that some of the particles display contrast due to complex internal structure. The particle indicated by an arrow in Fig. 2 is seen to contain three or four variants in the particle diameter of 3.4 nm. A still unresolved feature of the $t \rightarrow m$ transition in zirconia concerns twinning, which is commonly observed in monoclinic $ZrO_2$. Twins are believed to occur in bulk materials to accommodate, at least partially, the shape change associated with the $t \rightarrow m$ transformation [14–16]. Hence, such particles appear to contain twin-related variants or a mixture of hybrid crystals. However, it was reported that internal twins or coexisting hybrid crystals of the two phases were absent in fine particles of zirconia [17]. But in this investigation it is important to note that strong evidence was obtained to show that ultrafine particles of zirconia do contain internal twins or hybrid crystal phases or poly domains. These have also been reported in Ni and Au particles by Dhere *et al.* [18]. A particle size distribution histogram is plotted in Fig. 3. These particle sizes were measured from TEM micrographs. It appears that the particle size increases with an increase in calcination time. It is possible that sampling error may have played a role in the measurement. Nevertheless, the histogram in Fig. 3 provides a measure of the size distribution within the set of samples studied in this investigation. It is clear that the major number of particles is below 20 nm. The ultrafine particles are essentially spherical in shape.

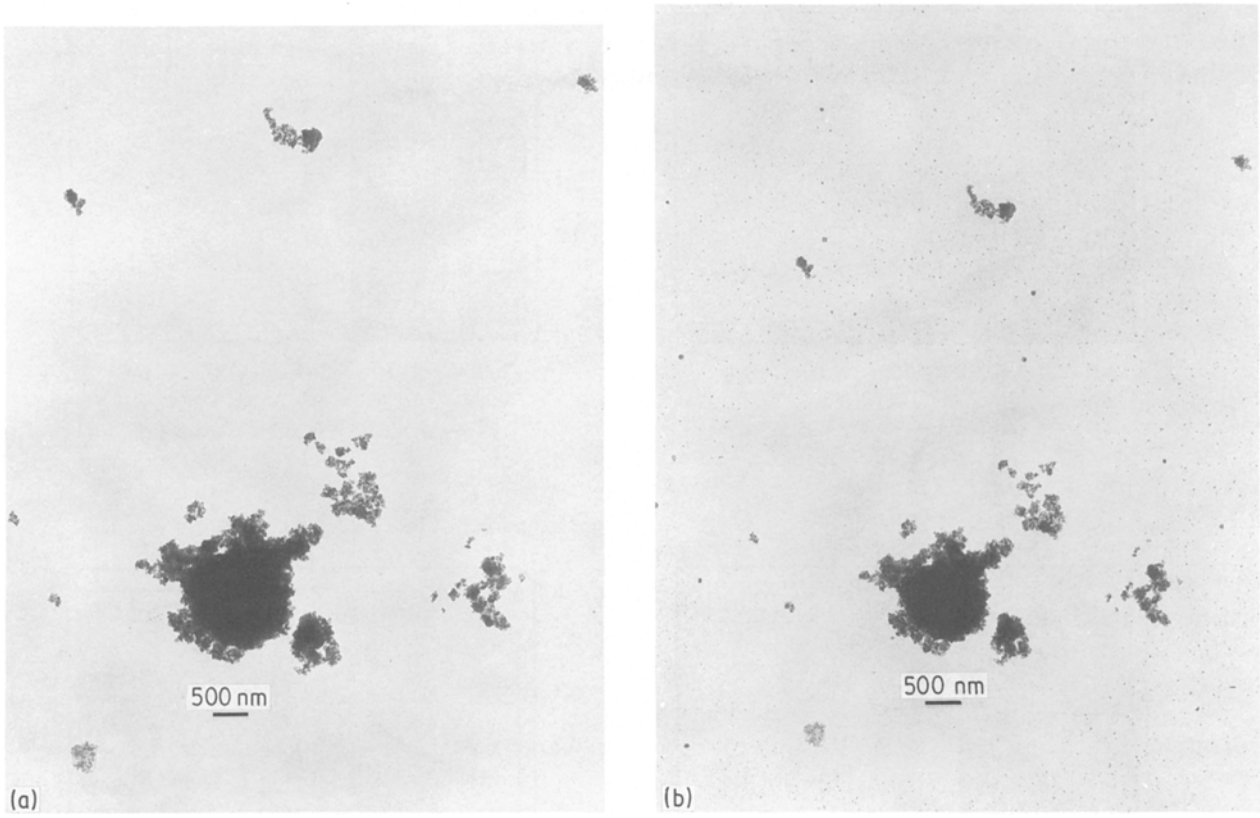


*Figure 1* (a) Bright field electron micrograph of an agglomerate or a lump before pulsing the beam, (b) the same area as (a) after pulsing the beam six times. The fine particles can be seen thrown out around the lump.

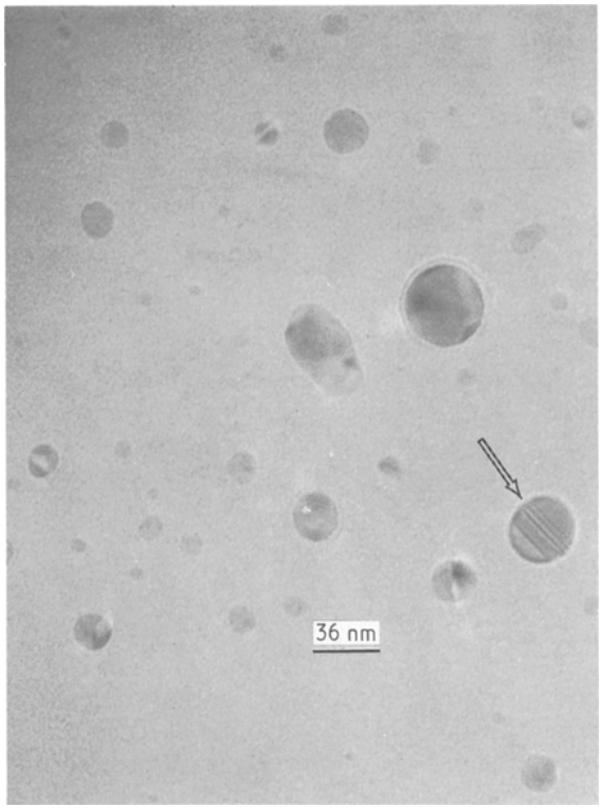


*Figure 2* Bright field electron micrograph from sample A. The particle marked by an arrow contains variants.

Electron microdiffraction patterns were obtained using a 2 nm probe in the conventional transmission mode from the particles shown in Fig. 4. The observed diffraction patterns were compared with those generated by theoretical calculations. The particles marked "a" and "b" are monoclinic particles aligned parallel to $[0\bar{1}0]_m$ and $[0\bar{1}1]_m$ zone axes, respectively, and show no substructure. However, the particle marked "c" in Fig. 4 shows substructure of polydomain nature. The microdiffraction pattern from this particle is shown in Fig. 5, wherein the crystal orientation is parallel to $[212]_t$ zone axis. The additional spots indicated by arrows in Fig. 5 are due to the existence of variants that occur during $t \rightarrow m$ transformation.

### 3.1.2. Sample B

This sample was calcined at 500 °C for 50 h and the X-ray diffraction data indicated the existence of 55% monoclinic phase. A considerable amount of tetragonal phase in Sample A has been transformed to monoclinic phase with calcination time.

A dark field micrograph obtained from this sample is shown in Fig. 6. The electron beam at 200 kV is condensed and spread over the agglomerate such that the fine particles are thrown out around the central agglomerate (Fig. 6). The particle size distributions obtained from this sample are plotted against the fraction cumulative frequency in Fig. 3. The major fraction lies in the range of 10–20 nm.

Microdiffraction patterns were obtained using a 5 nm probe from the particles marked in Fig. 7. Microdiffraction patterns obtained from these particles have been solved and are indicated in Fig. 8. Two typical diffraction patterns, one for tetragonal

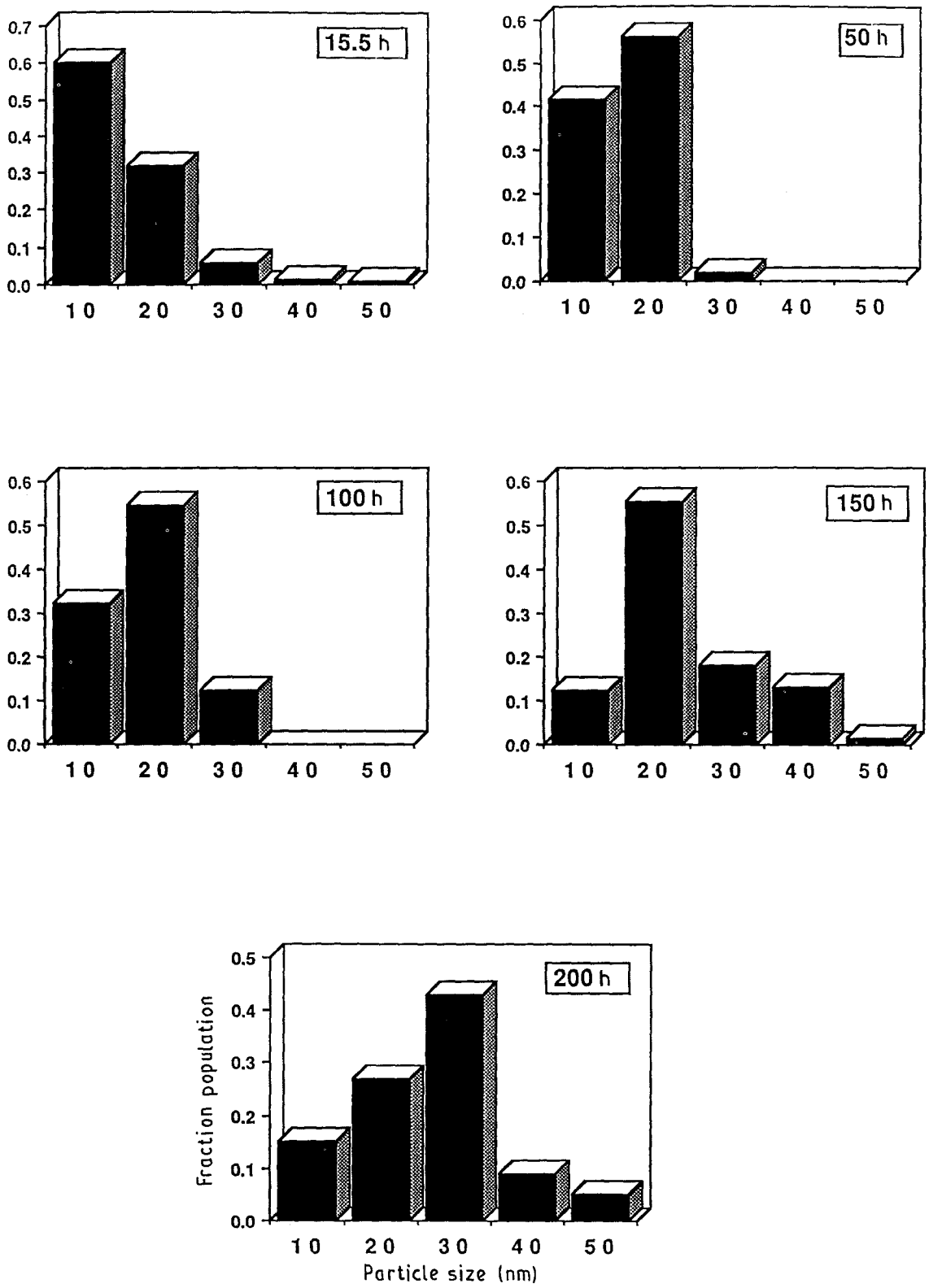


*Figure 3* Histogram showing particle size distributions for the samples.

and the other for monoclinic phases are shown in Fig. 8 with corresponding zone axis. Particle "P5" is a tetragonal particle aligned in [1 1 1] orientation as shown in Fig. 8a. It is to be noted that the particle P8 in Fig. 7, is a 6 nm particle whose diffraction pattern shows that it is the monoclinic particle aligned parallel to $[0\,1\,1]_m$ orientation (Fig. 8b). The diffraction patterns from all particles shown in Fig. 7 indicate that some of the particles are monoclinic particles and some of them are tetragonal. An interesting observation was made about the shapes of the particles. In Fig. 9, in addition to the existence of very fine particles of spherical shape, particles of hexagonal, pyramidal, icosahedron, rectangular, square, cone shapes are also evident. These shapes may have formed as the small particles cleaved off due to the thermal stresses developed in beam pulsing. It is worth noting that in addition to particles of different shapes, ultrafine particles of 1–10 nm in diameter which broke off from the larger particles are observed.

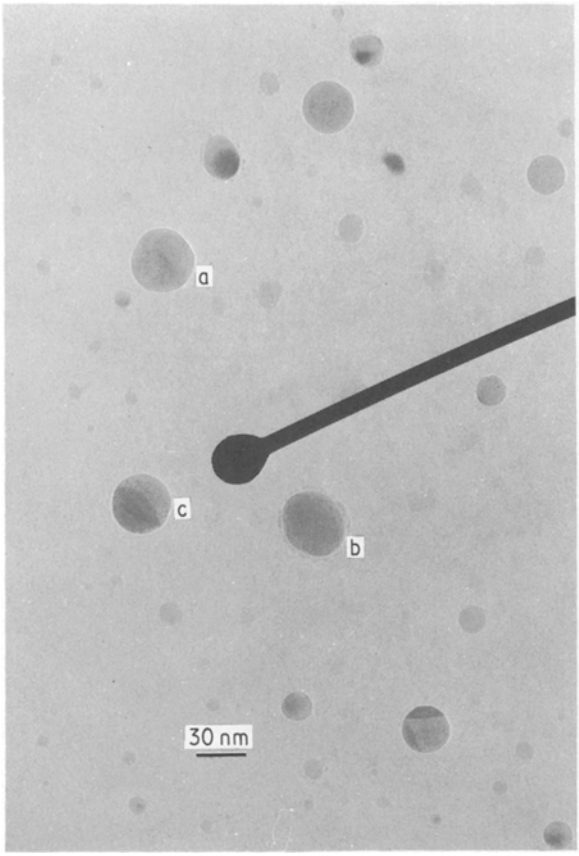


*Figure 4* Bright field electron micrograph from sample A. The particles "a" and "b" are in $[0\bar{1}0]_m$ and $[0\bar{1}1]_m$ orientations, respectively.

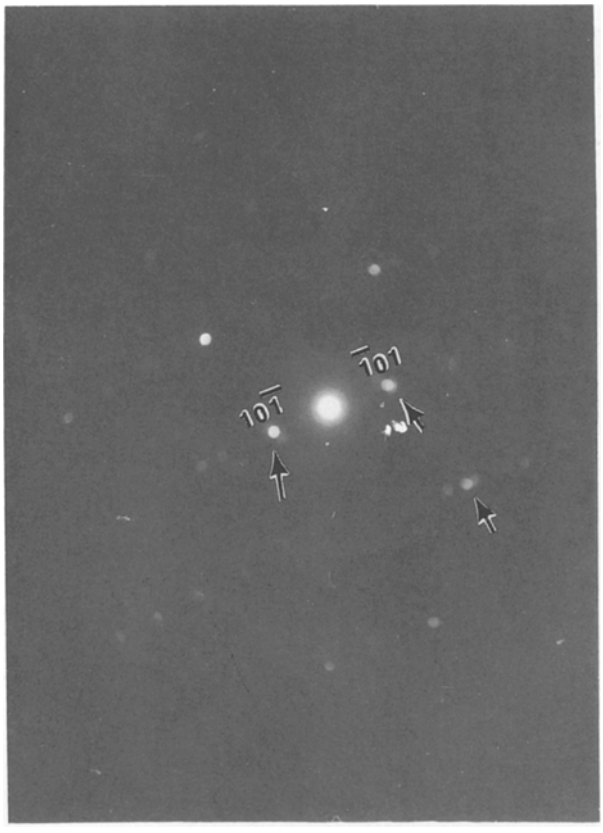


*Figure 5* The electron microdiffraction pattern of the particle "c" in Fig. 4. Primary reflections correspond to $[2\,1\,2]_t$ orientation. Four diffraction spots can be seen as indicated by arrows; these are due to the presence of 4 variants accompanying the $t \rightarrow m$ transformation.

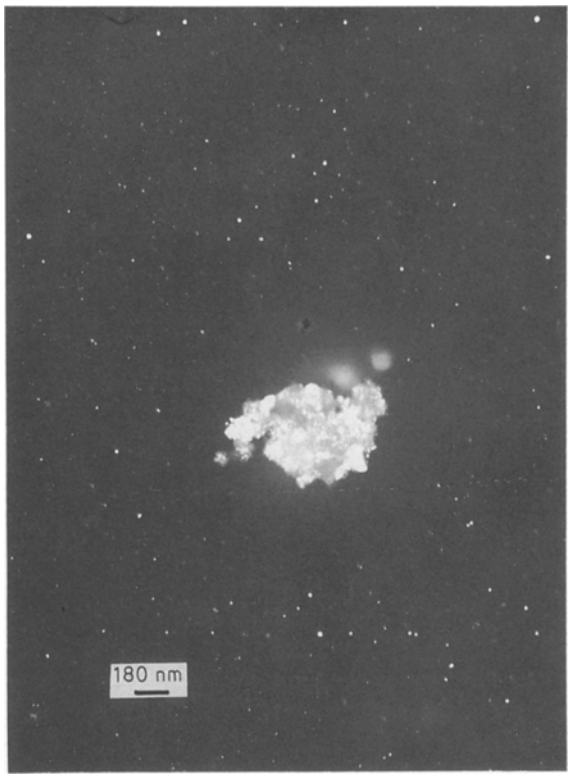


*Figure 6* Dark field electron micrograph from sample B, showing that the majority of particles are smaller than 10–20 nm.

### 3.1.3. Sample C

This sample was calcined at 500 °C for 100 h and on XRD analysis showed about 65% monoclinic phase. As expected the increase in calcination time has considerably aided the transformation from tetragonal to monoclinic phase [12].

Microdiffraction patterns using a 5 nm probe were obtained from various particles shown in Fig. 10. Particles of both the tetragonal and monoclinic symmetry were observed. Möire fringes were observed to exist in one of the particles shown in Fig. 10. In fact, these fringes produce an image of a dislocation.

### 3.1.4. Sample D

This sample was calcined at 500 °C for 150 h, and showed about 75% monoclinic phase (Table I). Microdiffraction patterns were obtained using a 5 nm probe from the various particles shown in Fig. 11; these indicated that there were several particles of tetragonal and monoclinic crystal structures.

### 3.1.5. Sample E

This sample, calcined at 500 °C for 200 h, showed about 85% monoclinic phase. The majority of tetragonal phase initially present after a 15 h calcination period was transformed to the monoclinic phase after a 200 h calcination period at 500 °C.

Microdiffraction data were obtained from five particles indicated in Fig. 12. A typical diffraction pattern is shown in Fig. 13a and the calculated pattern is presented in Fig. 13b. Most of the particles exhibit monoclinic symmetry consistent with our X-ray data.

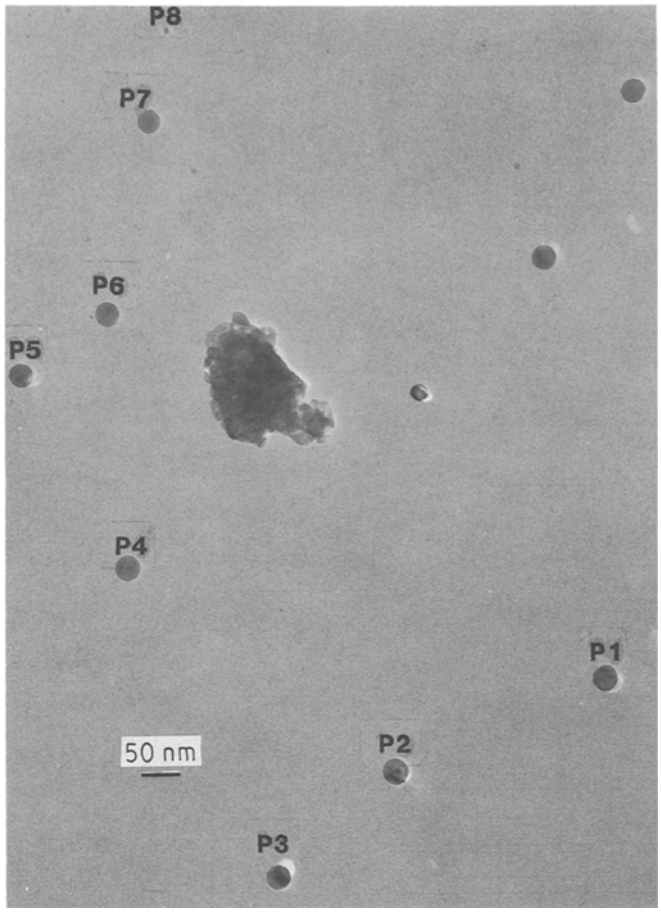


*Figure 7* Bright field electron micrograph from sample B. The orientations of the particles are: P1 = $[1\,1\,0]_t$; P2 $[1\,0\,2]_m$; P3 = $[1\,\bar{1}\,0]_m$; P4 = $[0\,1\,1]_m$; P6 = $[0\,1\,1]_t$; P7 = $[1\,1\,0]_t$.

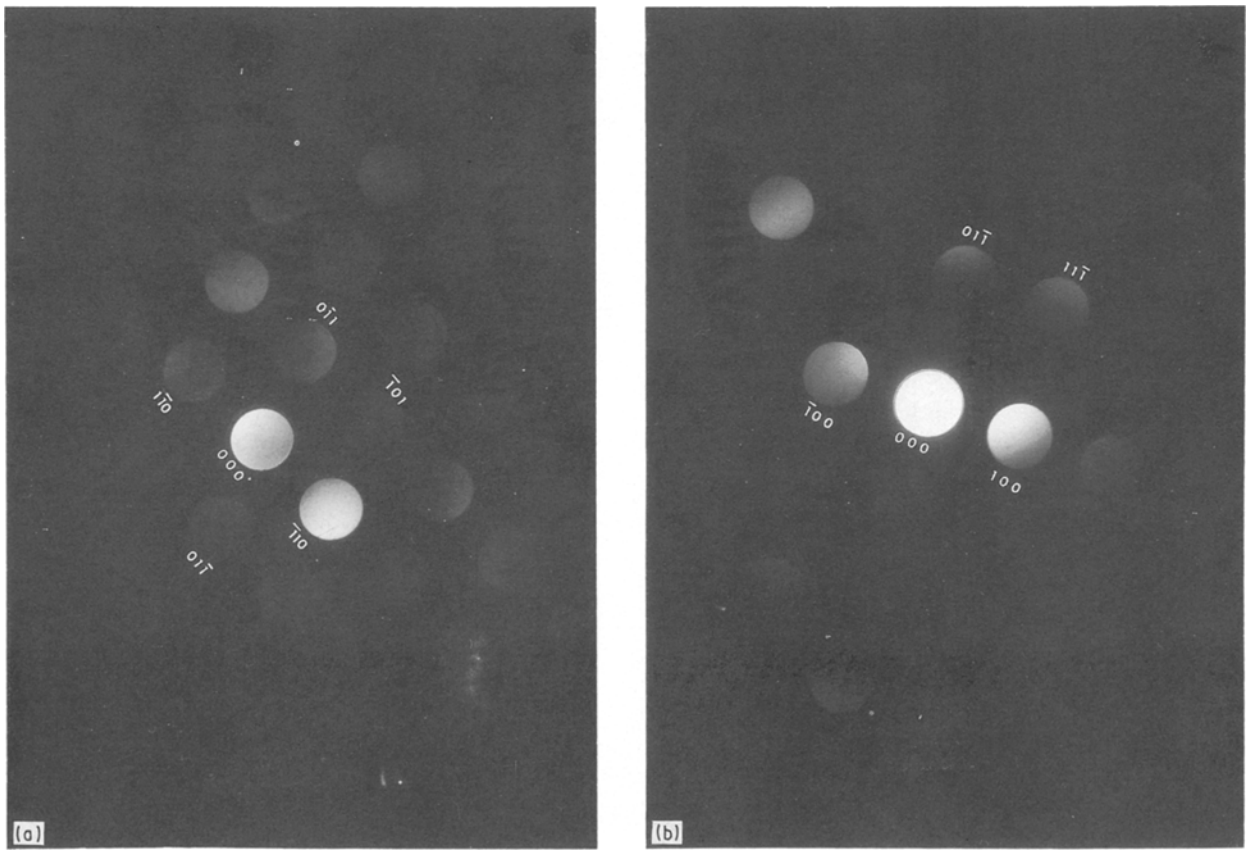


*Figure 8* (a) Electron microdiffraction using 5 nm probe from particle "P5" in Fig. 7 which has a $[1\,1\,1]_t$ orientation; (b) diffraction pattern from a 6 nm monoclinic particle "P8" which is parallel to $[0\,1\,1]$ zone axis.

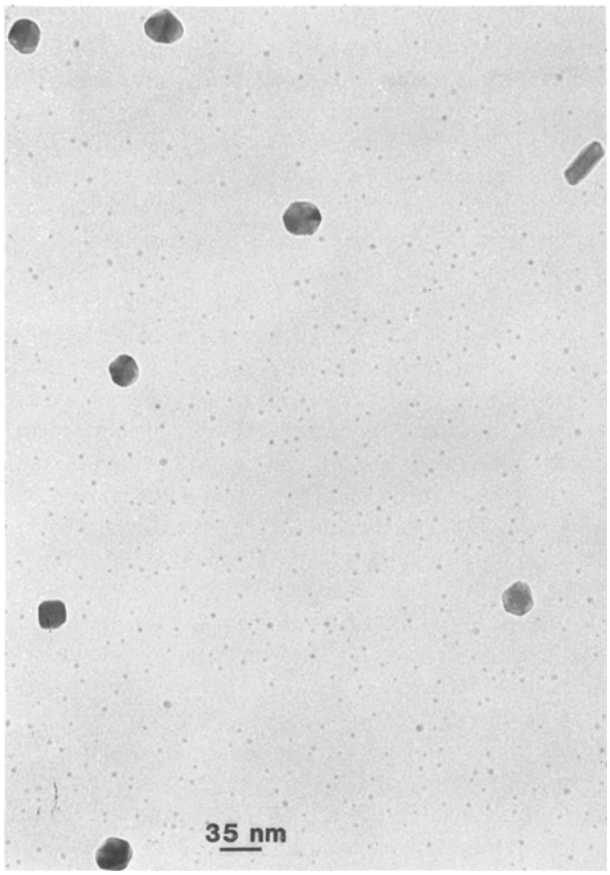


*Figure 9* Spherical zirconia particles of less than 10 nm in diameter. In addition, hexagonal, pyramidal, rectangular, square shapes of particles can also be seen.

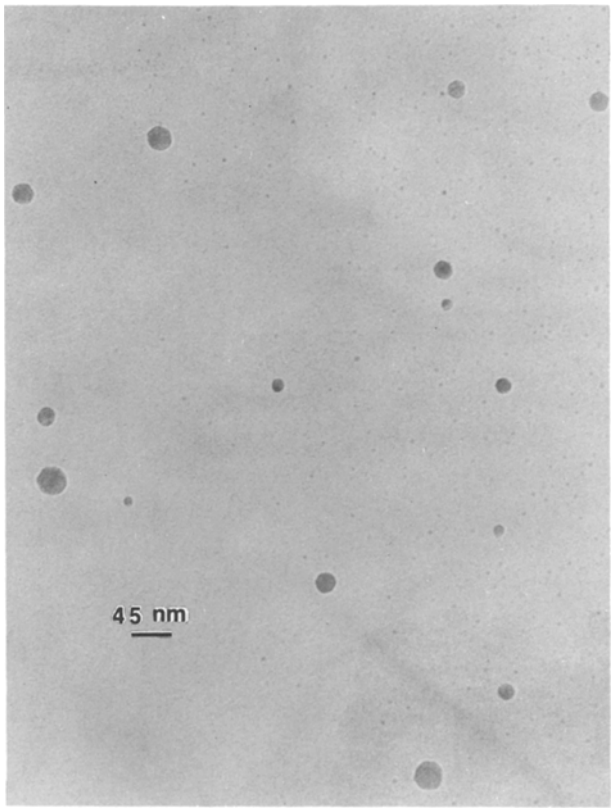


*Figure 11* Bright field electron micrograph from sample D. Again subnanometer zirconia particles less than 10 nm in diameter can be seen. Microdiffraction patterns were obtained from the particles which showed several monoclinic and a few tetragonal orientations.

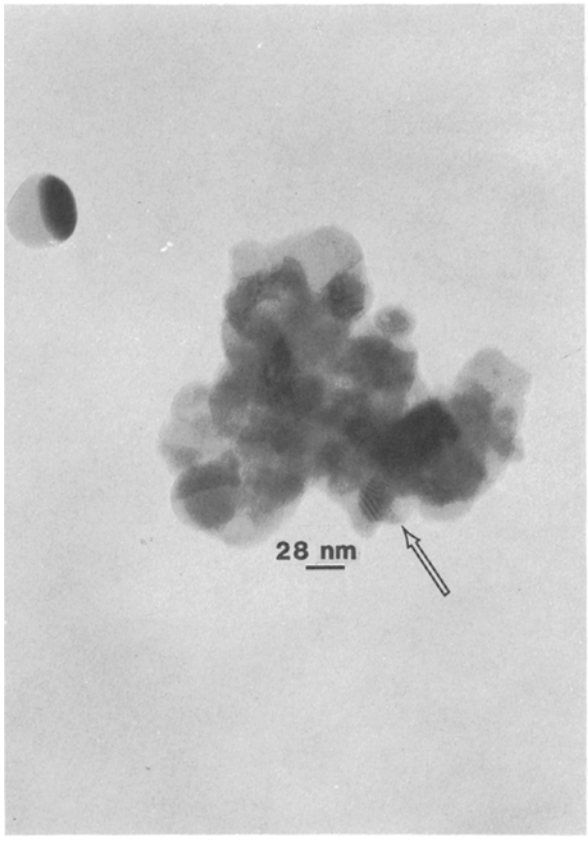


*Figure 10* Bright field electron micrograph from sample C. Möire fringes can be seen at the position indicated.

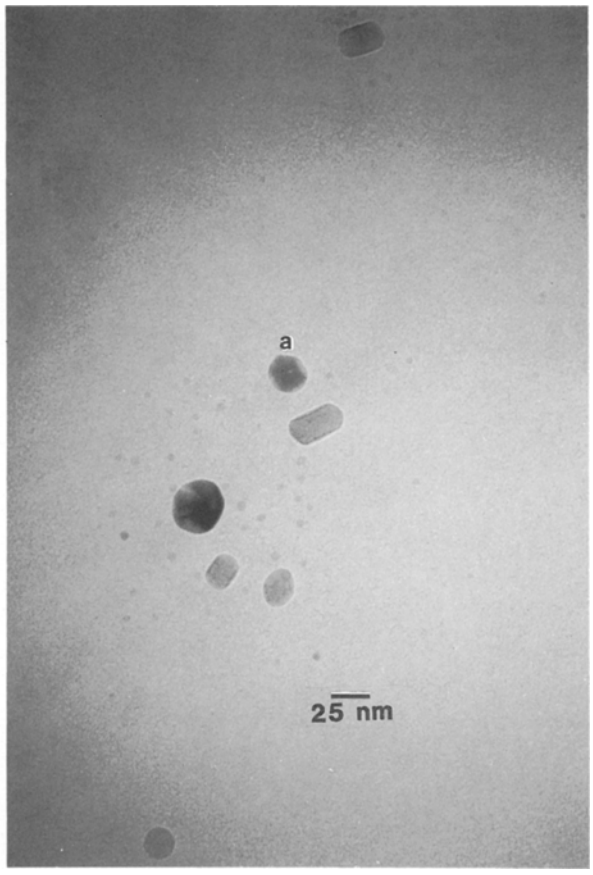


*Figure 12* Bright field electron micrograph image obtained from sample E, showing several particles.

Fig. 14 shows a few particles containing twins. An attempt was made to obtain microdiffraction patterns from the twinned particles using a 2 nm probe, however, it was not successful.

### 3.2. Crystallite Size Effect

Garvie [19, 20] proposed that the stabilization of tetragonal phase in zirconia at low temperatures depends on the crystallite size. If the crystallite size attains a critical value of 30 nm or above, the tetragonal → monoclinic transformation is favoured. This theory was questioned by the data of Morgan [21] among others [22–26] who was able to produce 6 nm monoclinic zirconia particles by extensive refluxing of zirconyl chloride solution at pH 1–2. We reported earlier that the precipitation of zirconia at pH 2–4 from zirconyl chloride solution produced ultrafine tetragonal zirconia particles with X-ray crystallite size of about 15–16 nm in size after calcination at 500 °C for 5 h. It was also reported that this tetragonal phase is transformed to monoclinic phase with increasing calcination time at 500 °C [12]. These earlier results made us question the crystallite theory proposed by Garvie [19, 20]. In this investigation, we have obtained further evidence from transmission electron microscopy that zirconia particles of as low as 6 nm or less exhibit monoclinic structure evinced by electron microdiffraction patterns. A 6 nm particle in Fig. 7 showed monoclinic symmetry in the microdiffraction patterns (Fig. 8b). Therefore, we believe that at low pH's ( < 4.0), the tetragonal structure arises from chemical factors. Rapid precipitation at these pH's somehow allow the polyzirconium species, and the associated water and OH ligands to form a *pseudo*-tetragonal structure, and this produces a tetragonal structure upon calcination at 500 °C. After calcining at 500 °C for longer periods of time, the

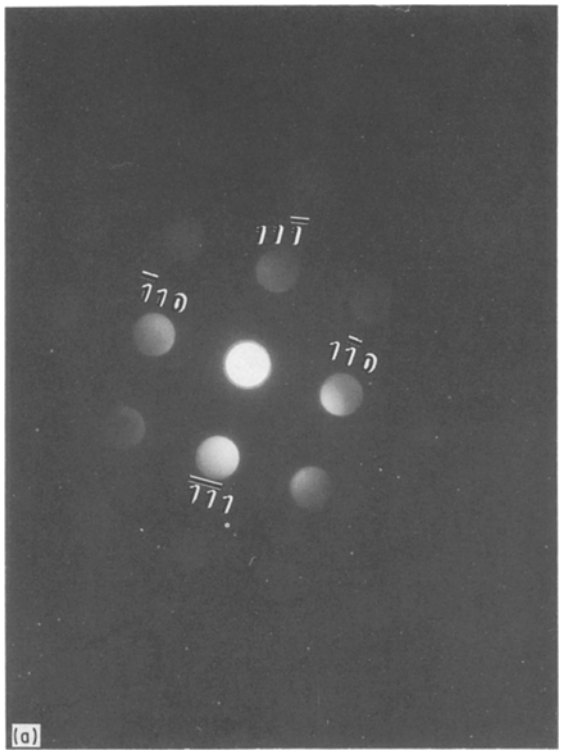


*Figure 13* (a) Electron microdiffraction pattern from the particle "a" in Fig. 12, (b) the pattern solved for $[1\,1\,2]_m$ orientation (observed reflections are indicated by '◬' and the calculated reflections are indicated by '△').

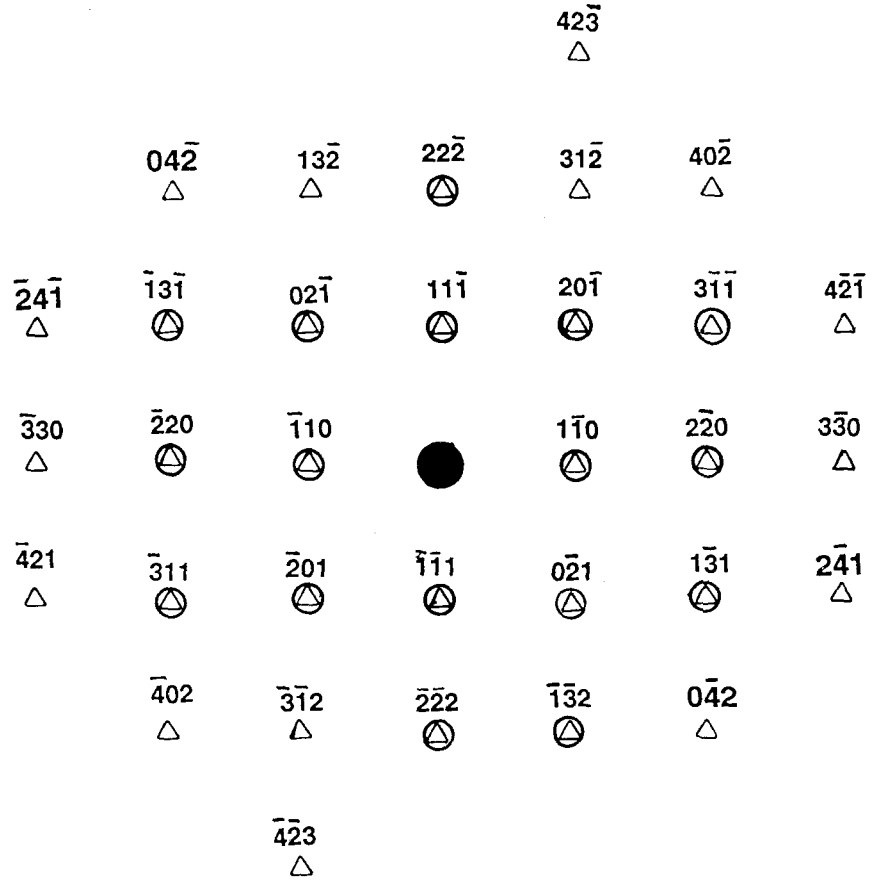

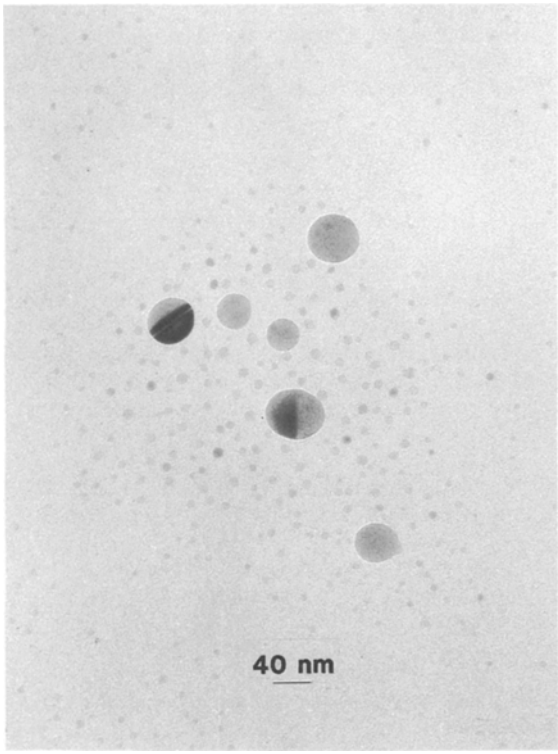


*Figure 14* Bright field electron micrographs showing twinned particles.

tetragonal structure transforms to a stable monoclinic structure by adjustments of atoms in the crystal lattices. In contrast, the tetragonal structure obtained at high pH's ( > 13) is quite stable at 500 °C even after 300 h of calcination [12]. The tetragonal structure developed at the high pH is a low-temperature stable phase, and the tetragonal structure developed at low pH's is destabilized, presumably by defects.

The $t \rightarrow m$ transformation in these fine particles is associated with twinning. These twins decrease the size of the diffracting crystallites in the monoclinic phase. Evidence is now available for the presence of subgrains and internal twins inside the 10–15 nm monoclinic particles which can easily account for the decrease in X-ray crystallite size in the $t \rightarrow m$ transformation. At the same time, it does not appear that the particles undergoing the $t \rightarrow m$ transformation increase significantly in physical size.

### 3.3. Ultrafine Particles in TEM and Microdiffraction

Microdiffraction is an effective tool in obtaining precise crystallographic data. This technique has certain advantages over selected area diffraction (SAD). The latter technique uses a wide beam (10–20 nm in diameter) and therefore the accuracy of the diffraction patterns from a particular region of interest is limited. On the other hand, microdiffraction technique utilizes a very narrow beam size (2–5 nm) and hence the diffraction patterns and the crystallographic information from them are more precise. Microdiffraction is a reliable method of obtaining diffraction data from subnanometer particles.

Earlier crystallite size or particle size distribution theories were based mostly on XRD average crystallite size. It is difficult to produce specimens which give images of separate, individual zirconia particles in electron microscopy. Those who produced ultrafine zirconia particles by sol-gel techniques were usually not able to precisely examine the particle sizes in TEM. For example, Pebler [27] prepared small zirconia particles by aerosol pyrolysis and reported that these fine particles were too thick to obtain TEM images. In our case, it appears that surface tension effects while evaporating the water or alcohol when preparing the microscope specimen cause the fine particles to join together to make an agglomerate too thick to permit one to obtain TEM images. In the present investigation, a technique to obtain individual zirconia particles of subnanometer size was devised. This technique involves searching an agglomerate or a lump and bring it to the centre of the microscope. Condensing and spreading the 200 kV electron beam on the lump causes the fine particles to be thrown apart. It is then easy to approach the individual subnanometer particles and to obtain microdiffraction patterns. We have observed this phenomenon for various catalyst samples in addition to zirconia. This technique is significant because it may provide a tool useful in obtaining individual fine particles in systems where it was difficult to obtain fine particles until now.

The point groups of cubic, tetragonal and monoclinic zirconias are $m\,3\,m$, $4/m\,m\,m$ and $2/m$, respectively. The point group symmetry decreases from cubic to tetragonal to monoclinic. The change from cubic ($m\,3\,m$) to tetragonal ($4/m\,m\,m$) is accompanied by a decrease in the order of symmetry from 48 to 16. This results in the occurrence of variants while the transformation occurs. The number of possible variants may be calculated by dividing the order of symmetry in the parent phase by that in the product phase [28]. Thus, in $c \rightarrow t$ transition in zirconia, $48/16 = 3$ variants are expected. This result was experimentally verified by Nagita [29], Heuer and co-workers [30, 31] and Sakuma [32]. Analogous conclusions can be derived for the $t \rightarrow m$ transition in zirconia. The orders of symmetry for tetragonal and monoclinic phases in zirconia are 16 and 4, respectively. Hence, the $t \rightarrow m$ transition must be accompanied by 4 variants ($16/4 = 4$). This was exactly the observed result in the present investigation. For example, in Fig. 2, the highlighted particle is seen to contain 4 variants. The microdiffraction pattern obtained from a particle marked "c" in Fig. 4, is shown in Fig. 5. The diffraction spots indicated by arrows in this figure clearly indicate the presence of 4 variants. Thus, strong evidence is obtained in this study for the existence of twin related variants in the individual zirconia particles.

## 4. Conclusions

A technique has been described which provides for the isolation of individual subnanometer particles in a catalytic material. Evidence was found in this investigation, in addition to our earlier XRD results, to suggest that crystallite size effect is not likely to be

responsible for the stabilization of tetragonal phase of zirconia at low temperatures. The ultrafine individual zirconia particles contain 4 twin related variants in accordance with Aizu's theory [28].

## References


1. O. RUFF and F. EBERT, *Z. Anorg. U. All. Chem.* **180** (1929) 19.
2. P. MURRAY and E. B. ALLISON, *Trans. Brit. Ceram. Soc.*, **53** (1954) 335.
3. C. T. LYNCH, F. W. VAHLDIEK and L. B. ROBINSON, *J. Amer. Ceram. Soc.* **44** (1961) 147.
4. R. N. PATIL and E. C. SUBBA RAO, *Acta Crystallogr.* **A26** (1970) 555.
5. H. S. MAITI, K. V. G. K. GOKHALE and E. C. SUBBA RAO, *J. Amer. Ceram. Soc.* **55** (1972) 317.
6. R. C. GARVIE, in "*High Temperature Oxides Part II*", edited by A. M. Alper (Academic Press, New York, 1970) p. 117.
7. A. H. HEUER and M. RUHLE, in "*Advances in Ceramics*", Vol. **12**, edited by N. Claussen, M. Ruhle and A. H. Heuer (American Ceramic Society, Columbus, 1984) pp. 1–13.
8. R. SUYAMA, T. ASHIDA and S. KUME, *J. Amer. Ceram. Soc.* **68** (1985) C314.
9. T. K. GUPTA, J. H. BECHTOLD, R. C. KUZNICKI, L. H. CADOFF and B. R. ROSSING, *J. Mater. Sci.* **12** (1977) 2421.
10. T. K. GUPTA, F. F. LANGE and J. H. BECHTOLD, *ibid.* **13** (1978) 1464.
11. B. H. DAVIS, *J. Amer. Ceram. Soc.* **67** (1984) C168.
12. R. SRINIVASAN, R. J. DE ANGELIS and B. H. DAVIS, *J. Mater. Res.* **1** (1986) 583.
13. R. SRINIVASAN, M. B. HARRIS, S. F. SIMPSON, R. J. DE ANGELIS and B. H. DAVIS, *ibid.* **3** (1988) 787.
14. J. E. BAILEY, *Proc. Roy. Soc. London Ser. A*, **A279** (1964) 395.
15. G. K. BANSAL and A. H. HEUER, *Acta Metall.* **20** (1972) 1281.
16. *Idem, ibid.* **22** (1974) 409.
17. T. MITSUHASHI, M. ICHIHARA and V. TATSUKE, *J. Amer. Ceram. Soc.* **57** (1974) 97.
18. A. G. DHERE, R. J. DE ANGELIS and P. J. REUCROFT, *Ultramicrosc.* **18** (1985) 415.
19. R. C. GARVIE, *J. Phys. Chem.* **69** (1965) 1238.
20. *Idem, ibid.* **82** (1985) 218.
21. P. E. D. MORGAN, *J. Amer. Ceram. Soc.* **67** (1984) C204.
22. R. CYPRÊS, R. WOLLAST and J. RAUCQ, *Ber. Duet. Keram. Ges.* **40** (1963) 527.
23. Y. MURASE and E. KATO, *J. Amer. Ceram. Soc.* **66** (1983) 196.
24. *Idem, ibid.* **62** (1979) 527.
25. J. LIVAGE, K. DOI and C. MAZIERES, *ibid.* **51** (1968) 349.
26. E. TANI, M. YOSHIMURA and S. SOMIYA, *ibid.* **66** (1983) 11.
27. A. R. PEBLER, *J. Mater. Res.* **5** (1990) 680.
28. K. AIZU, *Phys. Rev. B: Solid State*, **2** (1970) 754.
29. K. NAGITA, *Acta. Metall.* **37** (1989) 313.
30. V. LANTERI, R. CHAIM and A. H. HEUER, *J. Amer. Ceram. Soc.* **69** (1986) C258.
31. A. H. HEUER, R. CHAIM and V. LANTERI, *Acta Metall.* **35** (1987) 661.
32. T. SAKUMA, *J. Mater. Sci.* **22** (1987) 4470.



*Received 1 October 1990*
*and accepted 18 March 1991*